The EMBO Journal Vol.16 No.23 pp.6996–7007, 1997

Solution structure and basis for functional activity of stromal cell-derived factor-1; dissociation of CXCR4 activation from binding and inhibition of HIV-1

Matthew P.Crump, Jiang-Hong Gong[1], Pius Loetscher[2], Krishna Rajarathnam, Ali Amara[3], Fernando Arenzana-Seisdedos[3], Jean-Louis Virelizier[3], Marco Baggiolini[2], Brian D.Sykes[4] and Ian Clark-Lewis[1,4]

Protein Engineering Network of Centers of Excellence (PENCE) and Department of Biochemistry, 713 Heritage Medical Research Center, University of Alberta, Edmonton, Alberta, Canada T6G 2S2, [1]Biomedical Research Centre and Department of Biochemistry and Molecular Biology, University of British Columbia, Vancouver, British Columbia, Canada, V6T 1Z3, [2]Theodor-Kocher Institute, University of Bern, PO Box 3000, Bern 9, Switzerland and [3]Unite d'Immunologie Virale, Institut Pasteur, 75724 Paris Cedex 15, France

[4]Corresponding authors

The three-dimensional structure of stromal cell-derived factor-1 (SDF-1) was determined by NMR spectroscopy. SDF-1 is a monomer with a disordered N-terminal region (residues 1–8), and differs from other chemokines in the packing of the hydrophobic core and surface charge distribution. Results with analogs showed that the N-terminal eight residues formed an important receptor binding site; however, only Lys-1 and Pro-2 were directly involved in receptor activation. Modification to Lys-1 and/or Pro-2 resulted in loss of activity, but generated potent SDF-1 antagonists. Residues 12–17 of the loop region, which we term the RFFESH motif, unlike the N-terminal region, were well defined in the SDF-1 structure. The RFFESH formed a receptor binding site, which we propose to be an important initial docking site of SDF-1 with its receptor. The ability of the SDF-1 analogs to block HIV-1 entry via CXCR4, which is a HIV-1 coreceptor for the virus in addition to being the receptor for SDF-1, correlated with their affinity for CXCR4. Activation of the receptor is not required for HIV-1 inhibition.

Keywords: chemokines/G-protein coupled receptors/ nuclear magnetic resonance spectroscopy/protein synthesis/stromal cell-derived factor-1

Introduction

Stromal cell-derived factor-1 (SDF-1) was originally described as a secreted product of a bone marrow stromal cell line (Tashiro *et al*., 1993), and subsequently by expression cloning as a pre-B cell stimulating factor that partially replaced the need for stromal cells for the *in vitro* generation of B cells (Nagasawa *et al*., 1994). SDF-1 is a member of the chemokine family of pro-inflammatory mediators and is a potent chemoattractant for T cells, monocytes and lympho-hemopoietic progenitor cells. The expression of most chemokines is induced by cytokines, but SDF-1 is produced constitutively (Shirozu *et al*., 1995). Consistent with its *in vitro* activities, an *SDF-1 –/–* mouse has severely deficient myelopoiesis and lymphopoiesis (Nagasawa *et al*., 1996). The apparent effects of SDF-1 on early cells suggests that it could have unique functions such as in the trafficking or homing of lymphocytes and hemopoietic cells (Aiuti *et al*., 1996). Furthermore, both SDF-1 (Shirozu *et al.*, 1995) and its receptor (Federsppiel *et al*., 1993) are expressed widely outside the lympho-hemopoietic system suggesting that it could have fundamental roles in other tissues.

SDF-1 was found to be the ligand for a chemokine-like receptor (Bleul *et al*., 1996a; Oberlin *et al*., 1996), that had been identified previously and called HUMSTR (Federsppiel *et al*., 1993) or LESTR (Loetscher *et al*., 1994). It has been renamed CXC chemokine receptor 4 (CXCR4), following the conventions established for the nomenclature of chemokine receptors. This receptor has also been identified as a coreceptor (termed Fusin) for syncytia inducing (SI) forms of HIV (Feng *et al*., 1996). SDF-1 inhibits the entry and replication of SI forms of HIV-1 (Bleul *et al*., 1996a; Oberlin *et al.*, 1996). A distinct chemokine receptor CCR5 is a coreceptor for non-SI forms (Zhang *et al.*, 1996) and there appears to be a switch in coreceptor usage from CCR5 to CXCR4 during AIDS progression (Connor *et al*., 1997).

Chemokines are divided into two classes according to the relative position of the first two cysteine residues. In the CC chemokines, e.g. RANTES and monocyte chemoattractant protein-1 (MCP-1), the two cysteines are adjacent whereas in the CXC chemokines, e.g. interleukin-8 (IL-8) and growth related protein (GRO), the first two cysteines are separated by one residue (Baggiolini *et al*., 1997). The CC chemokines promote the recruitment of various types of leukocytes, whereas the CXC chemokines are more cell type-specific and activate predominantly neutrophils or T lymphocytes. SDF-1 belongs to the CXC family, but its average sequence identity with other human CXC chemokines and to the CC chemokines is only 27% and 22%, respectively. Its structural and functional relationship to other chemokines is unknown.

The human SDF-1 gene is located on chromosome 10 (Shirozu *et al*., 1995), whereas the other CXC chemokines are clustered on chromosome 4, and CC chemokines on chromosome 17 (Baggiolini *et al.*, 1997). Two alternatively spliced SDF-1 mRNAs encode SDF-1α (68 residues), and SDF-1β (72 residues); the four additional residues being located at the C-terminus (Shirozu *et al.*, 1995). A form that had been processed at the C-terminal end to generate a 67 residue protein was purified from stromal cells and we have called this form SDF-1 (Bleul *et al.*, 1996b). In contrast to other chemokines, which average 69% identity between human and mouse, SDF-1 is identical between

Fig. 1. The structure of SDF-1. (**A**) A stereoview of a superimposition of the 30 simulated annealing structures of SDF-1 on the average structure. The RMS deviation for residues 9–65 between all 30 structures and the average structure is 0.35 Å for backbone and 0.96 Å for heavy atoms. (**B**) A schematic diagram showing the restrained minimized average structure of SDF-1 created with the program MOLSCRIPT (Kraulis, 1991) and Raster3D (Merritt and Murphy, 1994).

these species, except for a single conservative change: Val to Ile at position 18 (Shirozu *et al.*, 1995). This identity suggests a fundamental role for SDF-1.

In this study we have determined the structure of SDF-1 and evaluated the structural requirements for its diverse activities. The solution structure of SDF-1 provides the basis for addressing the structural features which are essential for function. Many aspects of the molecular biology and physiology of SDF-1 are unique, so we cannot assume that rules established for other chemokines apply. For IL-8 the key receptor binding sites are in the N-terminal region and the loop succeeding the CXC motif, however, the two disulfide bridges are also important as they help provide the scaffold that stabilizes the active conformation (Clark-Lewis *et al.*, 1994; Rajarathnam *et al.*, 1994a). Structure–activity relationships of the chemokines studied to date indicate that this scaffold hypothesis is applicable to members of both the CXC and CC chemokine classes. SDF-1 antagonists were identified, which not only inhibited SDF-1 function, but also HIV-1 replication and thus indicating that receptor triggering is not required for inhibition of SI forms of HIV-1. On the basis of these studies we propose a two-step mechanism for the binding of SDF-1 and activation of CXCR4.

Results and discussion

Description of the solution structure of SDF-1

The solution structure of the 67 residue form of SDF-1 was determined from NMR data by the dynamic simulated annealing method (Nilges *et al.*, 1988) using the program X-PLOR (Brunger, 1993). Thirty structures were calculated that satisfied the NMR distance and angular restraints and a stereoview of the backbone atoms is shown in Figure 1A. The quality of the final structures is very high as judged by small deviations from idealized covalent geometry and good fit to the experimental NMR data (Table I). The structure of SDF-1 is well defined except for the N- and C-terminal residues, 1–8 and 66–67, respectively. SDF-1 adopts a chemokine-like fold consisting of three anti-parallel β-strands and an overlying

Table I. Structural statistics and atomic r.m.s. differences for 30 calculated SDF-1 structures

All (796)[a]	0.027 ± 0.001
Inter-residue (centre averaged)[a]	
Short ($1 < \|i–j\| \leqslant 5$)	0.039 ± 0.015
Sequential ($\|i–j\| = 1$)	0.024 ± 0.003
Long ($\|i–j\| > 5$)	0.029 ± 0.015
Inter-residue (R^{-6} averaged)[a]	
Long	0.025 ± 0.008
Intra-residue (centre averaged)[a]	0.020 ± 0.002
$i = j$	0.020 ± 0.008
E_{NOE} (kcal/mol)[b]	29.0 ± 1.9
E_{DIHE} (kcal/mol)[b]	1.49 ± 0.3
E_{REPEL} (kcal/mol)[b]	0.06 ± 0.05
Deviations from idealized geometry[c]	
Bonds (Å)	0.0031 ± 0.0001
Angles (°)	0.530 ± 0.008
Improper (°)	0.368 ± 0.007
Atomic r.m.s. differences (Å)[d]	
Backbone atoms (9–65)	0.35 ± 0.1
Heavy atoms (9–65)	0.96 ± 0.09

[a]The r.m.s. deviation of the experimental restraints (Å) is calculated with respect to the upper and lower limits of the input restraints.
[b]The values for E_{NOE} and E_{DIHE} are calculated from a square well potential with a force constant of 50 kcal mol^{-1} Å^2 and 200 kcal mol^{-1} rad^{-2}. E_{REPEL} is calculated with a force constant of 4 kcal mol^{-1} Å^{-4} and the final van der Waal's radii were set to 0.75 times the value used in the CHARMM force field.
[c]The values for bonds, angles and impropers show the deviation from ideal values based on perfect stereochemistry.
[d]R.m.s. differences of the 30 final simulated annealing structures superimposed on the average structure.

α-helix (Figure 1B). The well ordered regions include an extended loop (Arg12 to Ala19) which leads into a 3_{10} helix (Arg20 to Val23). The first β-strand (24 to 30) is connected by a type III turn (31 to 34) to the second β-strand (37 to 42) and the second and third β-strands (47 to 51) are connected by a type I turn (43 to 46). A type I turn (52 to 55) connects the third β-strand and the C-terminal α-helix (58 to 65).

SDF-1β, was also characterized by NMR and the data indicated that like SDF-1 it is well defined between residues 9 and 65. There was no significant change in either secondary or tertiary structure as a consequence of the five residue C-terminal extension that distinguishes SDF-1β from SDF-1.

SDF-1 and SDF-1β are monomers

Dimerization is a characteristic feature of chemokines (Fairbother and Skelton, 1996), and is not required for activation of the receptor (Rajarathnam *et al*., 1994b; Clark-Lewis *et al*., 1995). We therefore examined SDF-1 for its propensity to dimerize. Molecular weight determination by sedimentation equilibrium indicated that SDF-1 and SDF-1β are both monomers at physiological ionic strength and pH 5.0 and 7.0. In all CXC chemokines examined to date, the dimer interface involves the first β-strand. The absence of slowly exchanging amide protons for Leu26, Ile28 or Asn30 in the first β-strand of SDF-1 indicates that it does not form a CXC-like dimer interface (data not shown). In contrast, in most CC chemokines, the N-terminal region constitutes the dimer interface. However, the absence of slowly exchanging amide protons for the N-terminal residues and the observation of relatively intense peaks for both Val3 and Leu5 in the ^{15}N–^{1}H HSQC spectrum indicate that the N-terminal region is mobile, and not involved in inter-subunit interactions (data not shown). In addition, no NOE contacts analogous to those that are found in chemokine dimers of either CC or CXC class were detected. This suggests that both SDF-1 and SDF-1β are active as monomers.

Comparison of SDF-1 with other chemokines

Chemokine structures that have been solved to date have a common tertiary fold that consists of an N-terminal region, a loop region that follows the CXC or CC motif, three antiparallel β-strands in a Greek key like arrangement, and a C-terminal α-helix. Several structural features are unique to SDF-1 and distinguish it from other chemokines (Figure 2). Differences are apparent in the packing of the hydrophobic core and this is evident when we consider Trp57 which is highly conserved among CC chemokines and also present in IL-8. In SDF-1, Trp57 makes extensive NOE contacts with residues of the 3_{10} helix (Arg20, Val23), the first β-strand (Leu26), and the N-terminal loop (Val18). In contrast, in other chemokines, Trp57 is oriented away from the first β-strand and is packed predominantly against the side chains of residues in the N-terminal loop (Figure 2A). These differences in the hydrophobic core are reflected in the relative orientation of the α-helix to the rest of the protein: in SDF-1 it is aligned more parallel to the β-strands, whereas in all other chemokines it is orthogonal to the β-strands (Figure 2B, C and D). The packing requirements of the helix in SDF-1 are fulfilled by Trp57, Tyr61 and Leu62, which interact with residues of the first and second β-strands. Packing of the hydrophobic side chain of Leu55, which is part of the turn preceding the α-helix in SDF-1, also influences the hydrophobic core and the orientation of the helix. Interestingly, in all other chemokines, the residues at position 55 are smaller (e.g. Ala), and also tend to be either charged (e.g. Asp) or polar (e.g. Ser).

SDF-1 is a highly basic protein with 21% of the total residues being arginine, lysine or histidine. Analysis of the electrostatic potential at the molecular surface revealed further differences between SDF-1 and other chemokines (Figure 3). In SDF-1, positive surface charges are clustered along the first and second β-strands and the α-helix displays a predominantly negative surface charge. With CXC chemokines, a positively charged surface is clustered in the C-terminal α-helix, whereas the CC chemokines show no obvious pattern in the clustering of charges. The positive surface charge in IL-8 has been proposed to be critical for heparin binding (Rot *et al*., 1996). SDF-1 has been shown to bind heparin with higher affinity than either IL-8 or MCP-1 (Bleul *et al*., 1996b), suggesting that the surface charge distribution of SDF-1 could provide an optimal binding site for heparin or other cell-surface glycosaminoglycans.

N-terminal residues determine SDF-1 activity

To determine the structural requirements for function, the SDF-1 analogs described in Figure 4 were synthesized and assayed for their ability to bind SDF-1 receptors and to induce functional activation of the receptor by measuring induction of intracellular calcium levels. The results for all the analogs prepared in this study are summarized in Table II. In all chemokines studied to date, N-terminal

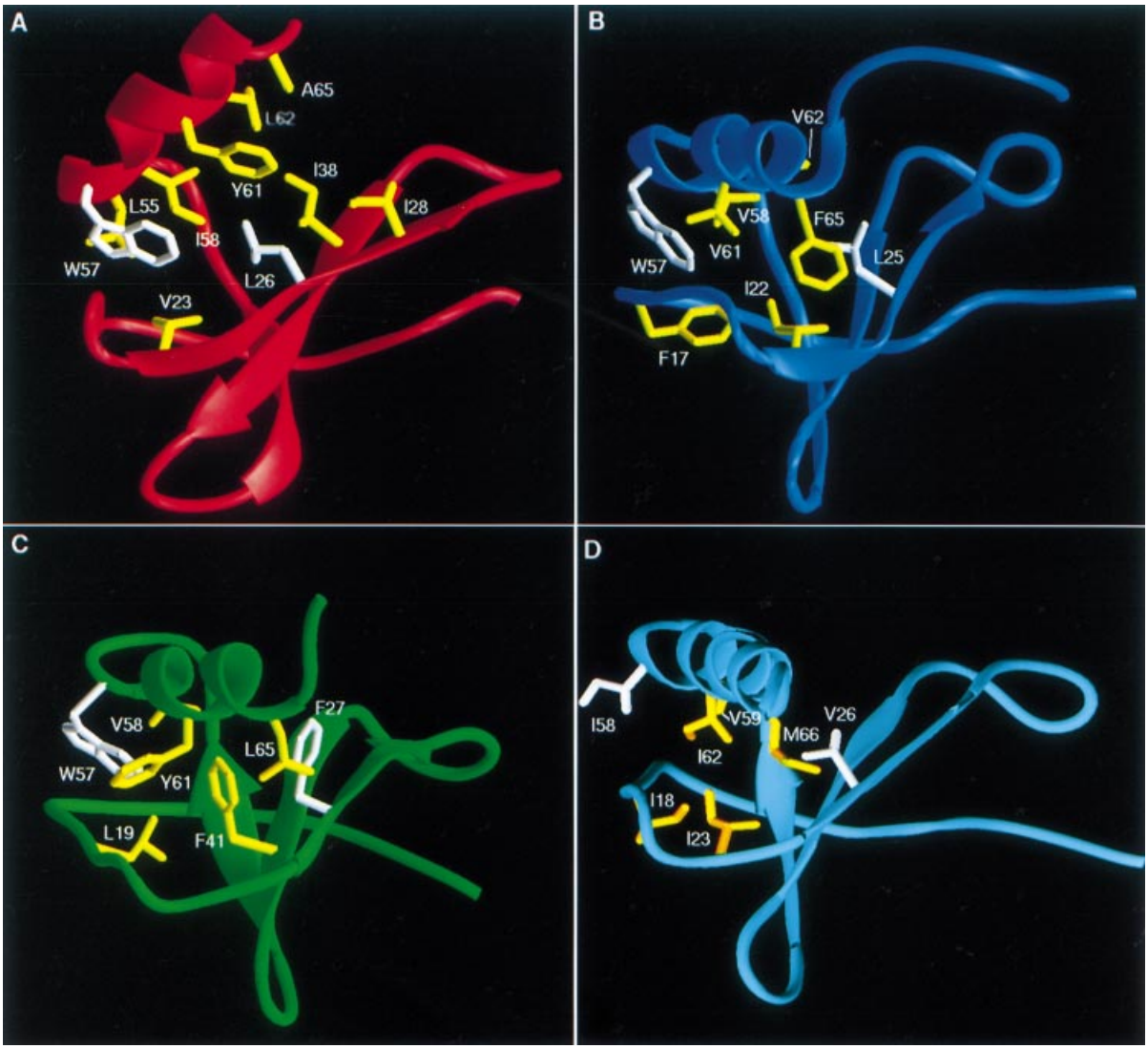

Fig. 2. Comparison of SDF-1 with other chemokines. Ribbon outlines of: (**A**) SDF-1; (**B**) IL-8 (Rajarathnam *et al.*, 1995); (**C**) RANTES (Fairbrother *et al.*, 1994); and (**D**) GRO (Skelton *et al.*, 1995). Trp57 and the residue that corresponds to Leu26 of SDF-1 are shown in white to indicate the difference in their relative positions. Residues 1 to 8 in SDF-1, 1 to 3 in IL-8, 1 to 7 in RANTES and 1 to 5 in GRO, are not shown for clarity.

residues preceding the first cysteine have been shown to be critical for both receptor binding and functional activation.

The role of the N-terminal region of SDF-1 was evaluated by preparing a set of analogs with sequential N-terminal truncations (Table II). SDF-1 (2–67), which is missing only the N-terminal lysine, lacked the ability to trigger CXCR4 signaling. Subsequent deletions resulted in analogs which were inactive. Despite their inability to induce receptor activation, two analogs 2–67 and 3–67, retained significant binding affinity for the receptor (Table II shows the K_ds of the analogs; a high affinity corresponds to a lower K_d). Thus the N-terminal residue is critical for receptor activation but not binding. To examine further the functional importance of residues 1 to 8, single substitution analogs of full-length SDF-1 were prepared. Two analogs with replacements of the N-terminal lysine were prepared, K1R, and one with ornithine, a non-natural amino acid which differs from lysine in being shorter by one methylene group. The K1R analog resulted in a dramatic loss in functional activity, but still retained binding, and thus was similar to 2–67 in its activity profile. However, the ornithine derivative retained significant binding and activity. This indicates that in SDF-1 an arginine at the N-terminal position cannot provide the necessary interactions to activate the receptor but the smaller ornithine side chain is tolerated. Determining the basis for the difference will require analysis of more analogs. Substitution of a glycine for proline at position 2 results in complete loss of activity, but affinity for the receptor is only ~3-fold less than native SDF-1. It is likely that the increased conformational flexibility of the glycine and/or the loss of interaction with the proline side-chain prevents the conformational change in the receptor that accompanies triggering. However, when the N-terminal region was extended by the addition of a glycine residue, the potency of the resulting analog, SDF–Gly (Figure 4), was higher than native SDF-1. This suggests that the alpha amino group of native SDF-1 is not important for function, and therefore the lysine side chain is likely to form the critical interactions. Furthermore, the results suggest that the backbone of the N-terminal region is partly exposed,

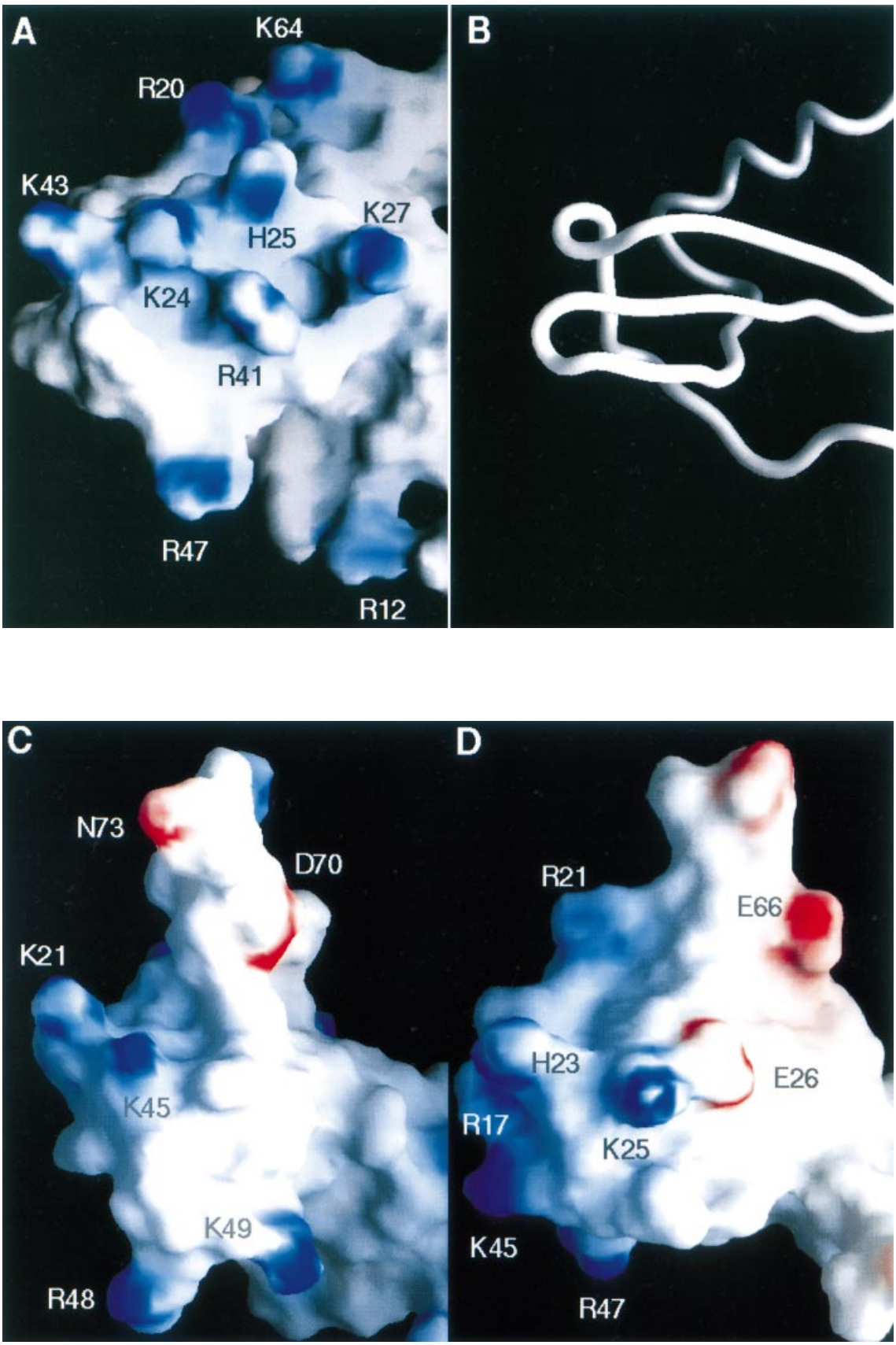

Fig. 3. Comparison of the surface charge distribution of chemokines. Shown is the surface electrostatic potential of: (**A**) SDF-1; (**C**) GRO; and (**D**) RANTES. (**B**) A tracing of the backbone of SDF-1 with the same orientation as (A), (C) and (D). A section of the first and second β-strands with the first strand running from left to right is shown in each panel. The electrostatic potential at the surface was calculated using the Poisson–Boltzman equation implemented in GRASP (Nicholls *et al*., 1991). Colors indicate the calculated electrostatic potential, with blue for positive and red for negative charge.

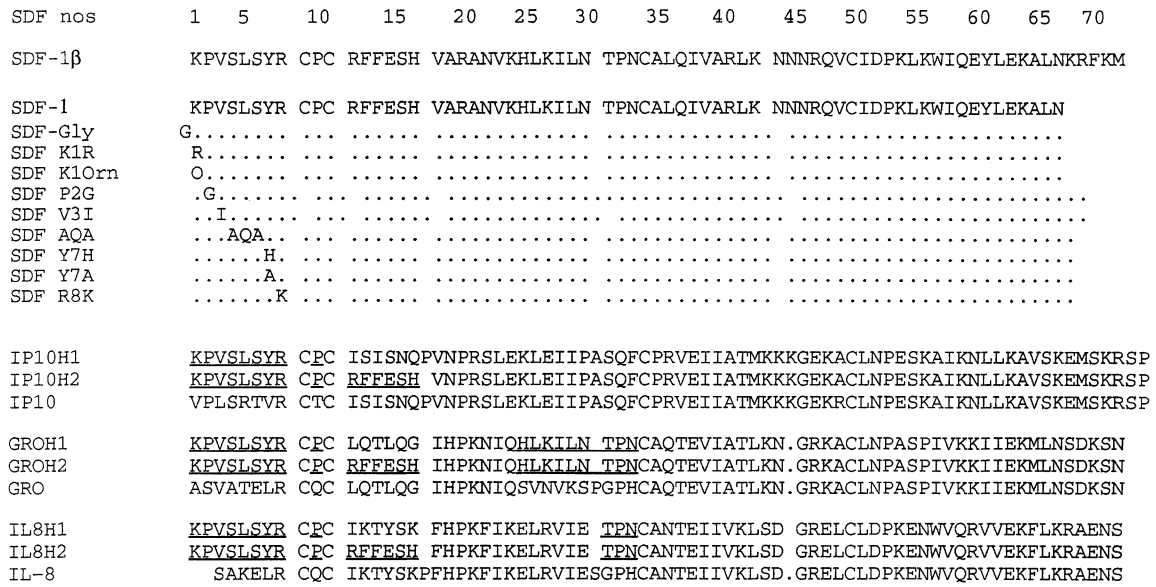

Fig. 4. Sequence alignment of SDF-1 analogs. Shown are the sequences of SDF-1β, SDF-1 (67 residue form), and the indicated analogs. SDF-1/chemokine chimeras are given the appropriate chemokine name followed by H1 or H2. For the chimeras the parts of the sequence corresponding to SDF-1 are underlined. The parent chemokines are given for comparison. GRO is also termed GROα or MGSA (Baggiolini *et al*., 1997).

because, if the N-terminus is buried then it would not accommodate additional residue(s). Thus, in these experiments four analogs were identified; 2–67, 3–67, K1R and P2G, with high affinity for the receptor, but with low receptor signaling. All four analogs had modifications of the lysine and/or proline suggesting that these two residues comprise the receptor activation motif of SDF-1. Of the four only P2G induced no detectable signaling, and as this analog had the highest binding affinity (Figure 5 and Table II), it was selected for studies aimed at determining its antagonist properties. P2G inhibited SDF-1-induced chemotaxis of CEM cells (Figure 5C).

The effects of substitutions in the 3 to 8 region in the N-terminal region were less dramatic, and the potency of the analogs approximately corresponded to their binding affinity. Interestingly, the potency of SDF-1 V3I was increased ~3-fold compared with native SDF-1. As with SDF–Gly, the binding of the V3I analog was slightly higher than native SDF-1, but the difference was not significant. This suggests that the introduction of isoleucine, which has a larger non-polar side chain, facilitates receptor activation. The findings with this analog and SDF–Gly suggest that the activity of native SDF-1 can be enhanced. Thus, despite the conservation of the SDF-1 structure between species, SDF-1 can readily accommodate changes to its structure, suggesting the feasibility of engineering analogs or small molecule ligands with high affinity.

Residues 4, 5 and 6 were changed simultaneously in the analog [A4, Q5, A7] SDF-1, and activity was significantly decreased relative to native SDF-1. Binding was also decreased but only ~3-fold. Thus these residues are not essential for binding or function, but they affect the ability of the N-terminal residues to induce activation. To examine the role of tyrosine 7 analogs with histidine or alanine replacements were prepared. Both analogs were active, but Y7H was almost fully potent, whereas the Y7A was significantly weaker than SDF-1. This suggests that it is unlikely that the tyrosine forms specific bonding interactions to the receptor, and its role is more likely to be steric and/or conformational. SDF-1, like other CXC chemokines, has an arginine immediately preceding the N-terminal cysteine. Because the integrity of this arginine is essential for chemokine binding to CXCR1 and CXCR2 (Clark-Lewis *et al*., 1995), we prepared an SDF-1 analog with a conservative replacement. This analog, R8K, had only an ~5-fold lower potency and binding affinity indicating that in contrast to other CXC chemokines, arginine was not absolutely required.

To analyze further the role of the N-terminal region in determining SDF-1 function we designed chimeras of SDF-1 with other CXC chemokines; interferon-inducible protein-10 (IP10), IL-8 and GRO. These chemokines are functionally unrelated to SDF-1 and bind different receptors. The relatively low similarity of SDF-1 with these chemokines suggests that chimeras can be used to determine whether alternative chemokine frameworks can provide the required context for the N-terminal region of SDF-1. In addition, by 'cutting and pasting' additional SDF-1 residues to generate more complex chimeras, a role for other regions of SDF-1 can be identified. This chimera approach has been successfully used for defining the structural elements of chemokines that are important for function (Clark-Lewis *et al.*, 1994). The sequences of the chimeras characterized in this study are shown in Figure 4.

A GRO hybrid with the N-terminal region of SDF-1 (1–8) (GROH1, Figure 4) was prepared and assayed for SDF-1 activities. Surprisingly, GROH1 was only 7-fold less active than SDF-1 in inducing calcium. This hybrid also had residues 25–33 which includes the β-turn between β-strands 1 and 2, as this had been shown to be a conformational requirement for IL-8 and the two molecules share structural similarity (Figure 2). However, subsequent experiments demonstrated that this turn is not critical for SDF-1 activity (not shown). A construct, IP10H1, that

Table II. Summary of SDF-1 structure–activity studies

Analog[a]	$[Ca^{2+}]_i$ EC30 (nM)[b]	Binding K_d (nM)[c]	HIV IC_{50} (nM)[d]
SDF-1	1.1	3.6 ± 1.6	79
SDF-1β	1.0	2.2 ± 1	40
SDF1 2–67	>10 000(A)	20 ± 9	UD
SDF1 3–67	UD(A)	46 ± 11	UD
SDF1 4–67	UD	340 ± 112	UD
SDF1 5–67	UD	390 ± 210	UD
SDF1 6–67	UD	410 ± 134	UD
SDF1 7–67	UD	470 ± 6	UD
SDF1 8–67	UD	490 ± 269	UD
SDF1 9–67	UD	UD	UD
SDF–Gly	0.3	3 ± 0.8	79
K1R	>10 000(A)	13 ± 7	794
K1Orn	5.4	5.8 ± 3.5	631
P2G	UD(A)	9 ± 1	562
V3I	0.3	2.7 ± 1.5	63
AQA	25	9 ± 5	355
Y7A	7.8	15 ± 0	708
Y7H	3.5	3.2 ± 0.7	112
R8K	4.5	18 ± 7	794
IP10H1	154	917 ± 118	ND
IP10H2	6.5	57 ± 25	UD
IP10	UD	UD	UD
GROH1	7.5	51 ± 11	ND
GROH2	1.1	10 ± 1	446
GRO	UD	UD	UD
IL8H1	>10 000	UD	UD
IL8H2	10 000	UD	UD
IL8	UD	UD	UD

[a]The sequences for the indicated analogs are shown in Figure 4.
[b]The effective concentration for 30% of maximum (EC30) rate of induction of intracellular free calcium was determined from the dose–response curves.
[c]The dissociation constants (K_d ± SD) are the mean of three different competition binding experiments.
[d]The analogs were titrated in the HIV infectivity assay and the HIV inhibition was determined by titration of each analog.
UD, undetectable; ND, not done; A, antagonist.

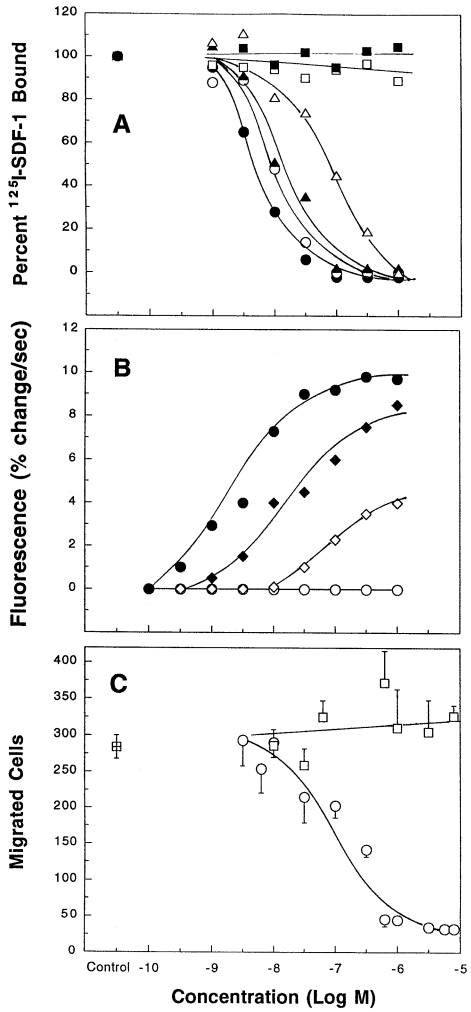

Fig. 5. Functional activity of SDF-1 analogs. (**A**) Receptor binding of SDF-1 analogs. Competition binding for [^{125}I]SDF-1 of: SDF-1 (●); P2G (○); GROH1 (△); GROH2 (▲); GRO (□); and SDF-1 (1–8) (■). Non-specific binding was subtracted and the results are presented as a percentage of maximal c.p.m. bound in the absence of competitor. (**B**) Induction of intracellular free calcium by SDF-1 analogs. Shown is the rate of change of fluorescence of Fura-2, a vital dye with a calcium dependent fluorophore, at the indicated concentration of SDF-1 (●); IP10H1 (◇); IP10H2 (◆); and P2G (○). (**C**) Chemotaxis inhibition by SDF-1 analogs. SDF-1 (3 nM) was added to all the bottom wells, and P2G (○) and SDF-1 (9–67) (□), were added to the bttom wells at the indicated concentrations. The control (⊞) is with SDF-1 alone.

had only the N-terminal region and Pro10 of SDF-1 had significant SDF-1 activity (Figure 5B), suggesting that it is the N-terminal region of SDF-1 that is important. The proline between the first two cysteines (the X in CXC) was included in all the chimeras. The role of this residue is yet to be determined but the nature of the side chain does not appear to be important for other CXC chemokines (Clark-Lewis *et al.*, 1994). In contrast a similar IL-8 chimera (Figure 4) with the SDF-1 N-terminus and the turn of SDF-1 (31–33) was inactive. Nevertheless, the results with the GRO and IP10 chimeras demonstrate the importance of the N-terminal region in determining receptor binding and activity and suggest that it is the major functional determinant of SDF-1.

Because of the critical role of the N-terminal region of SDF-1 in receptor activation and function, the activity of peptides corresponding to the N-terminal segment were evaluated. Two peptides, SDF-1 (1–8) and SDF-1 (1–9), had no detectable chemoattractant activity (not shown) or binding to CEM cells. The results for binding of SDF-1 (1–8), are shown in Figure 5A. In addition they did not show synergy with the truncated analogs in binding or in chemotaxis (not shown). Thus the peptides do not assume the conformation(s) necessary for binding to the receptor, implying that the protein scaffold, and/or receptor binding sites, is important for determining the optimal conformation of the N-terminal region for it to bind to the receptor.

Identification of a second binding site: the RFFESH motif

The chimeras with the N-terminal domain of SDF-1 were active, but less potent than native SDF-1. To test whether additional residues of SDF-1 are required for maximal potency we made further chimeras. The loop region that links the CXC motif to the 3:10 turn (Figure 2) is required for receptor binding of IL-8 (Clark-Lewis *et al.*, 1994), and for selectivity for CXCR1 and CXCR2 (Lowman *et al.*, 1996). Residues 12–17 (the RFFESH sequence) in

the corresponding loop region of SDF-1 (Figure 1) have some unusual features compared with the corresponding region of other chemokines. For example, residue 12 is an arginine, whereas a hydrophobic residue is usually found at this position and is important for activity of CXC chemokines. The remainder of the loop, except for Phe14, is solvent-exposed. To determine the effect of this region an IP10 chimera (IP10H2), with the RFFESH motif and the N-terminal domain of SDF-1, was synthesized (Figure 4). The potency of IP10H2 was 21-fold higher than IP10H1, which did not have the RFFESH motif (Figure 5B and Table II). Furthermore, the binding affinity was 16-fold higher. Compared with native SDF-1, the IP10H2 chimera was 6-fold less potent and had 14-fold lower affinity. A GRO chimera (GROH2) that contained both the N-terminal region and RFFESH, was equivalent to SDF-1 in potency, but had ~3-fold lower affinity for CXCR4. The RFFESH motif resulted in an ~5-fold increase in the binding of the chimera. The corresponding IL-8 chimera was inactive. Chemokine chimeras containing only RFFESH from SDF-1 have not been tested. However, as the results in Table II indicate that there is an absolute requirement for the N-terminal region for binding and activity, it is unlikely that the RFFESH motif alone would lead to activity in the absence of the N-terminal region. The results with the chimeras indicate that the N-terminal region and the RFFESH region contain the contact residues that are essential for fully functional SDF-1.

The results with the chimeras indicate that the structural core of SDF-1 can be substantially replaced by the framework of two other chemokines that have only 17% (IP10) or 25% (GRO) identity with SDF-1. The failure of the IL-8 structural core to support SDF-1 binding could be due to incompatibilities (e.g. steric or electrostatic) between the new framework in the chimera and CXCR4. The functional difference between native SDF-1 and the GRO and IP10 chimeras could be due to either slight incompatibilities between the new framework and CXCR4, or suboptimal conformation of the binding motifs. It is paradoxical that features of the three-dimensional structure, that distinguish SDF-1 from other chemokines, are not critical for binding or activation of CXCR4. However, we have only examined *in vitro* assays that are sensitive to interactions with CXCR4, and therefore these structural features of SDF-1 may be required for interactions with physiologically important partners other than CXCR4. For example, the clustering of positive charges in SDF-1 is apparently not critical for CXCR4 binding, because the two other chemokine core structures have different charge distributions yet support the functional motifs of SDF-1. However, it is possible that the positively charged surface is important for binding to heparin or other glycosaminoglycans. This could be important for SDF-1 physiology, but in this study we have focused on *in vitro* activities that result from CXCR4 activation, and therefore the structural features that are involved in interactions with other *in vivo* substrates have not been addressed.

Inhibition of HIV-1 by SDF-1 agonists and antagonists

The ability of native SDF-1 to inhibit HIV-1 replication arises because the virus has adopted CXCR4 (fusin) as a coreceptor for HIV-1 entry into target cells (Bleul *et al.*, 1996a; Oberlin *et al.*, 1996). To determine the HIV-1 inhibition by the SDF-1 analogs indicated in Table II, they were tested using $CD4^+$ HeLa cells and a SI HIV-1 isolate. The readout measured the transcriptional activity of viral LTR driven constructs, as the induced transcription of viral genes has been shown to correlate with level of infection. The concentration required for 50% of maximal inhibition (IC_{50}) was 80 nM for SDF-1. SDF-1β was consistently ~2-fold more potent in its inhibitory activity. The antagonist analog, PG2, inhibited HIV-1, and its weaker potency compared to SDF-1, reflected its lower affinity for CXCR4 (Figure 6). The K1R antagonist analog also had significant inhibitory activity. Thus the most potent SDF-1 agonists and antagonists inhibited SI HIV-1. Taking into account all the analogs that had significant inhibitory potency (Figure 6B and Table II), there was a strong correlation with binding affinity for CXCR4, but not with induction of signaling.

The observation that SDF-1 antagonists inhibit HIV-1 entry is in keeping with findings that CC chemokine antagonists inhibit entry of NSI forms of HIV-1. In general, HIV inhibition by the SDF-1 analogs correlated well with

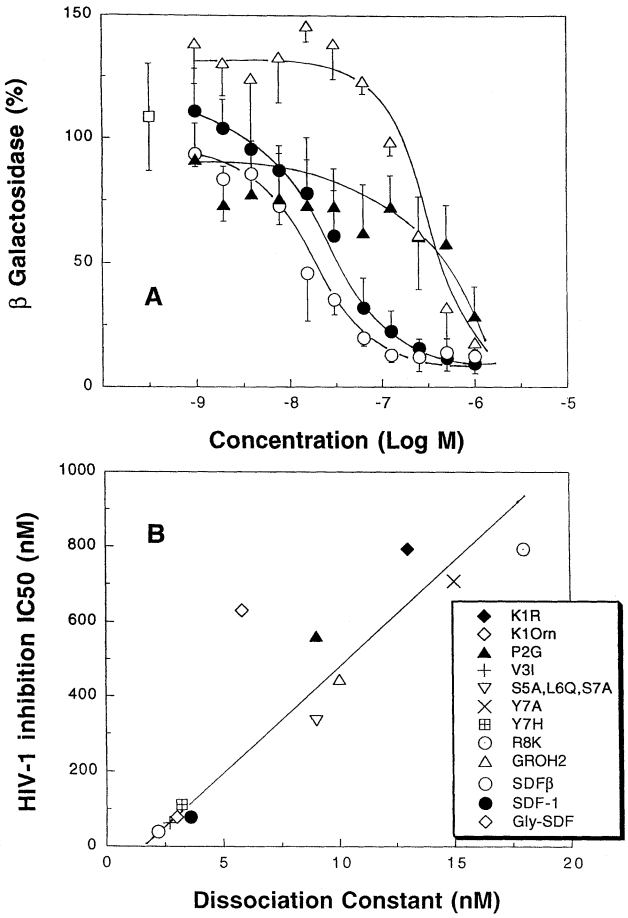

Fig. 6. Effect of SDF-1 analogs on HIV-1 replication: correlation with receptor binding. (**A**) The inhibition of HIV-1 by SDF-1 (●); SDF-1β (○); P2G (▲); and GROH2 (△). The control (□) had no chemokine added. (**B**) Correlation of HIV inhibition with binding. The IC_{50} values for HIV-1 inhibition are plotted against the K_d values for the indicated analogs. The IC50 and K_d values (Table II) were calculated from the titration curves for inhibition of HIV-1 and binding, respectively.

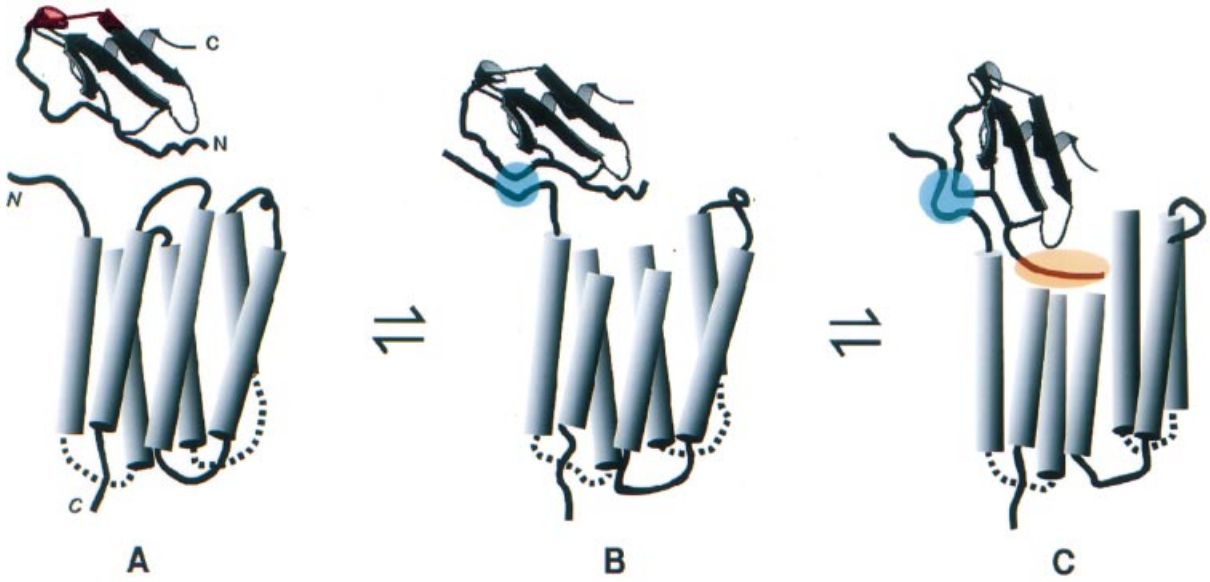

Fig. 7. A model for interaction of SDF-1 with CXCR4. A schematic depicting the interaction of SDF-1 with the receptor is shown. CXCR4 is shown with the seven helices represented as cylinders, which are connected by the surface and cytoplasmic loops. The N-terminal and C-terminal segments of the receptor, and the N- and C-terminus of SDF-1, are annotated as N and C. SDF-1 is shown as a MOLSCRIPT diagram. (**A**) indicates the receptor and ligand separately prior to any interaction between the two. (**B**) indicates interaction of the SDF-1 RFFESH loop (site 1) with the N-terminal segment of the receptor. The contact region is shown in blue. Two of the helices are truncated [compare with (A)] to highlight the binding groove of the receptor. (**C**) Shows the N-terminal region (site 2) of SDF-1 bound in groove at the top of the helices (orange). Binding of the N-terminal region results in activation of the receptor, which is depicted in (C) by the change in conformation of the receptor helices compared with (B).

their affinity for CXCR4. However, the concentration of SDF-1 required for inhibition was 40–80 nM, which is significantly higher than that required for receptor signaling or binding. The concentration of RANTES required to inhibit NSI HIV-1 was significantly higher than the receptor K_ds (Arenzana-Seisdedos *et al.*, 1996). Many factors are likely to affect this including the viral isolate, the length of time it has adapted to tissue culture, and the cells used. Furthermore it is likely that a higher level of receptor occupancy is required for HIV-1 inhibition than for receptor signaling. The binding results (Figure 5A) indicate that at a concentration of SDF-1 of 80 nM, which gives 50% inhibition of HIV-1, CXCR4 is almost saturated. The basis for the requirement for saturation is likely to be the complex kinetics of the interaction between the virus and its coreceptors; the gp120 must interact with both CD4 and CXCR4, but only a few gp120 coreceptor contacts are required for entry. This means that close to maximal occupancy would be needed to prevent multipoint attachment to the cell, and hence entry of the virus.

The results with the antagonist indicate that signaling is not required for HIV-1 replication. The molecular mechanism of inhibition of viral entry is not yet clear. It seems likely from these results that the virus is using the CXCR4 as an anchoring site rather than mimicking the function and hence binding of SDF-1. It is unlikely that the binding sites for SDF-1 and the gp120 are the same, but they could overlap. SDF-1 could inhibit by a steric hindrance mechanism that prevents interaction with the receptor. It is noteworthy that SDF-1β, which is bulkier because of the extra C-terminal residues, was 2-fold better than SDF-1 at inhibiting virus. However, addressing the question of the nature of the viral CXCR4 binding sites will require further studies.

A model for SDF-1 receptor interactions

Based on these results we propose a two site model for SDF-1 binding to CXCR4 (Figure 7). Our two-site model for SDF-1 receptor interactions is also compatible with current knowledge of the structure–function of other chemokines, and we suggest that it will be a general model for this family of chemoattractants. A two-site model has been proposed for C5a, an unrelated mediator that binds a distinct seven transmembrane segment receptor (Siciliano *et al.*, 1994). The two receptor binding sites are contained in SDF-1 (1–17) that has the sequence: KPVSLSYR-CPC-RFFESH. The results show that the RFFESH site is important for optimal binding, but is not sufficient for receptor activation, and we hypothesize that this region (site 1) makes the initial contact with the receptor (A to B). We suggest that this step serves as an initial SDF-1 docking step, and this step could be like a key that permits access to the more buried receptor site. In the subsequent step (B to C), the N-terminal residues bind to a groove amongst the helices, which induces a change in the conformation of the receptor transmembrane helices that allows intracellular G-protein binding and signaling of cellular function (Farrens *et al*., 1996). The N-terminal region (site 2), which is disordered in solution, becomes structured during binding and establishes contacts with the receptor groove. Nevertheless, addition of a Gly residue to SDF-1 did not affect activity and some of the N-terminal residues could be modified with minimal change in function. This suggests that the bound form of the N-terminal region is not completely buried within the transmembrane region, but rather is bound in a shallow site.

Receptor activation requires Lys-1 and Pro-2 within the N-terminal region. Modifications to Lys-1 and Pro-2 result in antagonists because the variants can no longer induce the conformational change in the receptor that is required

for activation. Changes to other residues result in functional molecules of variable potency, and therefore it seems that only the Lys Pro is directly involved in receptor activation. Structure–function studies of the IL-8-related chemokines indicate that a three residue motif, ELR, is the activation motif (Clark-Lewis *et al.*, 1994). Like SDF-1, for MCP-1, MCP-3 and RANTES the N-terminal two residues comprise the activation site (Gong *et al*., 1996; J.-H.Gong and I.Clark-Lewis, unpublished). All chemokines studied have separate binding sites, which are located either side of the CXC or CC motif, although the precise extents of these sites have not been determined in all cases.

We have proposed that the N-terminal region of CXCR4 interacts with the RFFESH of SDF-1, by analogy with other chemokine receptors. Thus, for CXCR1, CXCR2 and CCR2 an important role for the N-terminal region has been demonstrated (LaRosa *et al*., 1992; Monteclaro and Charo, 1996). For IL-8, the loop site corresponding to the RFFESH of SDF-1, binds the N-terminal segment of the receptor (LaRosa *et al.*, 1992). The details of the nature of the binding pocket are unknown and therefore a variation of the model whereby other surface loops participate in ligand binding, as is the case with CCR5 (Farzan *et al*., 1997), has not been excluded.

Future experiments based on this model will lead to a more detailed understanding of the molecular mechanisms of the interaction of SDF-1 and HIV-1 with CXCR4. Nevertheless this study has provided the basis for the design of second generation SDF-1 agonists and antagonists with potential uses in bone marrow transplantation and AIDS.

Materials and methods

Chemical synthesis

SDF-1, SDF-1β and all the SDF-1 and chemokine related proteins were synthesized by step-wise solid phase methods using tBoc protection chemistry. After hydrogen fluoride deprotection, the polypeptides were folded, purified as described previously (Clark-Lewis *et al*., 1994). [^{15}N]Val and [^{15}N]Leu were incorporated as the isotopically labeled tBoc derivative (Cambridge Isotope Laboratories, Andover, MA). Purity of the products was assessed by ion-exchange HPLC and mass spectrometry. The measured mass of each of the final products, as determined by electrospray mass spectrometry, was consistent with the average mass calculated from the atomic composition.

Sedimentation equilibrium ultracentrifugation

These studies were carried out on a Beckman Spinco Model E analytical ultracentrifuge using absorbance optics. Sedimentation runs were carried out at a concentration of ~0.5 mg/ml in 50 mM sodium phosphate, 100 mM sodium chloride and at pH 5 and 7. Molecular weights from sedimentation data were determined as described previously (Rajarathnam *et al.*, 1994b). The data indicated a single mass species and the calculated molecular weights for SDF-1 (7800 at pH 5.0; and 7800 at pH 7.0) and for SDF-1β (8500 at pH 5.0; 9000 at pH 7.0), within experimental error, were consistent with the expected weight for the monomers (SDF-1 = 7835; SDF-1β = 8526).

NMR spectroscopy

NMR experiments were performed on a Varian Unity 600 MHz and Varian Inova 500 MHz spectrometers at 30°C. Samples for NMR were 2 mM protein, in ^2H_2O or 90% H_2O/10% ^2H_2O, containing 20 mM sodium acetate, 1 mM sodium azide and 1 mM DSS, pH 4.9. ^{1}H resonances were assigned from standard two-dimensional pulse sequences (Wuthrich, 1986). Ambiguities in chemical shift assignments and overlap of the cross-peaks in the 2D-TOCSY and NOESY experiments were resolved by collecting ^{1}H NMR data at different temperatures (20–40°C), salt conditions (0–200 mM NaCl) and from the following 2D and 3D heteronuclear experiments: natural abundance [^{13}C]HSQC and ^{13}C-edited HMQC-NOESY on a 4 mM protein sample in ^2H_2O; ^{1}H–^{15}N HSQC and 3D ^{15}N-edited NOESY-HSQC of a [^{15}N]Val and [^{15}N]Leu-labeled SDF-1 (Zhang *et al*., 1994).

Structure calculations

NOE cross-peak intensities were classified as strong, medium, weak or very weak, corresponding to upper distance restraints of 2.8, 3.5, 4.0 and 5.0 Å respectively, on the basis of 50 ms and 150 ms NOESY spectra. These were distributed as 188 long range, 82 medium range, 240 sequential and 256 intra-residue NOEs. Upper limits for non-stereospecifically assigned methyl and methylene protons were corrected appropriately with center averaging. In addition, 0.5 Å was added to the upper boundary to correct for higher intensity for distances involving methyl protons. Restraints involving aromatic ring protons were treated with $<R^{-6}>$ averaging. Backbone ϕ angles were calculated from a high resolution DQF-COSY spectrum. Stereo-specific assignments and χ^1 restraints were obtained from the analysis of the $^3J_{\alpha\beta}$ coupling constants in DQF-COSY spectrum and the relative intensities of the NOEs from the NH and the C_α to C_β protons in a 50 ms NOESY spectrum collected in D_2O. χ^2 torsion angles for leucine residues were obtained from analysis of intra-residue NOEs between the C_α and $C_{\delta1}$ and $C_{\delta2}H$ protons after establishing the correct χ^1. Hydrogen-bonding restraints were identified on the basis of observing slow exchanging amide protons in a TOCSY spectrum recorded within 4 h of dissolving the protein in D_2O.

The solution structure of SDF-1 was determined using the dynamic simulated annealing method using the program X-PLOR (Nilges *et al*., 1988; Brunger, 1993). A total of 770 inter-proton distance, 93 dihedral angle and 34 hydrogen-bond restraints were used in the structure calculations corresponding to 15.2 restraints per residue for the well ordered region (9–65) of the protein. In the final 30 structures there were no NOE violation >0.3 Å or dihedral angle violations >5°. Analysis of the (ϕ,ψ) backbone torsion angles using the program PROCHECK (Lakowski *et al.,* 1991) revealed that for the structured region (residues 9 to 65), 85% of residues were in the most favored 'core' region of the Ramachandran plot, and 15% were in the 'allowed' region.

Cytosolic free calcium measurements

Phytohemagglutinin activated human peripheral blood lymphocytes or CEM cells, a human T cell line, was used for SDF-1 assays. Cells were loaded with Fura-2 acetoxymethyl ester (0.4 nmol per 10^6 cells), then washed and stimulated with a chemokine, and the change in fluorescence was recorded as a function of time and the rate of change in the $[Ca^{2+}]_i$ determined (von Tscharner *et al*., 1986).

Chemotaxis assay

Cell migration was evaluated by using Boyden microchambers (Neuro-Probe, Cabin John, MD). Samples were diluted into RPMI medium containing BSA (10 mg/ml) and HEPES (25 mM). Twenty-five μl samples were added to the bottom well of micro Boyden chambers. The wells were covered with a polycarbonate Nucleopore filter (3 μm pore size) and then 50 μl of a suspension of CEM cells (5×10^6/ml) was added to the upper wells suspended in the above buffer. After 2 h at 37°C in a humidified atmosphere, cells that had migrated into the bottom wells were counted. All determinations were performed in triplicate. The background was the mean number of cells migrating in medium alone.

^{125}I-labeling of SDF-1 and receptor binding

An extensive search was conducted for cell lines that gave reproducible saturable binding. Although CXCR4 is very widely expressed, we found that most cells, including activated T cells, from peripheral blood, Jurkat T cells, CXCR4-transfected HEK 293 cells, had high levels of non-receptor-specific binding. SDF-1 is extremely basic (pI 11.5), and platelet factor 4, which is another basic chemokine-related protein, also had high non-specific binding, suggesting that this feature could be the basis for this observation.

The CEM T cell line was found to give reliable saturable SDF-1 binding and was used for all the binding studies. This line has been also used for assays of CXCR4 mediated HIV-1 infection (Gervaix *et al*., 1997). The binding of the analogs was determined by competition for binding of ^{125}I-labeled SDF-1. SDF-1 was labeled using lactoperoxidase. One mCi (3.7 Mbq) of Na^{125}I (ICN, Biomedicals, Irvine, CA) and 1 μg of lactoperoxidase (80–150 U/mg; Sigma Chemical Co., St Louis, MO) were added to 5 μg of SDF-1, in 50 μl of 0.5 M sodium acetate, pH 6.5, at room temperature for 3 min. To stop the reaction saturated tyrosine (150 μl) was added and the labeled SDF-1 was separated from the free label by Sephadex G-25 chromatography. For binding assays, cells

(2×10^6) were maintained at 4°C for 30 min in the presence of 4 nM ^{125}I-labeled SDF-1, and increasing concentrations of unlabeled competitor (10^{-10} to 10^{-5} M), in 200 µl RPMI medium, containing HEPES (25 mM), BSA (10 mg/ml) and sodium azide (0.1%). The cell-associated c.p.m. was determined by immediately separating the cells through a 2:3 mixture of diacetylphthalate and dibutylphthalate. The specifically bound c.p.m. were calculated by subtracting the non-specifically bound c.p.m. (the c.p.m. bound in the presence of 100-fold molar excess of unlabeled SDF-1) from the total c.p.m. that was bound to the cells. Dissociation constants (K_d values) were determined by Scatchard analysis.

HIV-1 replication

Assays were performed using a clonal CD4$^+$ HeLa cell line with a stably integrated *lacZ* gene under the control of the HIV-1 LTR (Clavel and Charneau, 1994). This CD4$^+$ LTR-lacZ cells, 1.5×10^4 per well in 96 microtiter trays, were cultured with 250 µl infectious supernatants of HIV LAI in the presence of various concentrations of test SDF-1 analog in triplicate. After 24 h β galactosidase was measured in cell lysates. Cells were lysed in 100 µl of a buffer containing 0.125 % NP-40, 60 mM Na_2HPO_4, 40 mM NaH_2PO_4, 50 mM 2-mercaptoethanol, 2.5 mM EDTA and 100 µl of 80 mM sodium phosphate pH 7.4, 10 mM $MgCl_2$, 50 mM β-mercaptoethanol, and then 6 mM chlorophenol red–β galactopyranoside monosodium salt added. The mixture was incubated for 20 min at 37°C and the absorbance at 570 nM measured.

Acknowledgements

Correspondence should be sent to either I.C.-L. or B.D.S. The authors thank P.Lavigne, B.Dewald, B.Moser, M.Wolf and M.D'Apuzzo for valuable discussions. We acknowledge L.Vo, J.Anderson, P.Owen, P.Borowski and M.Williams for technical assistance in the synthesis and characterization of the proteins; G.McQuaid and B.Lix for maintenance of NMR spectrometers; L.Kay for pulse sequences; and L.Hicks and C.M.Kay for the sedimentation equilibrium studies. I.C.-L. is the recipient of a Scientist award from the Medical Research Council of Canada.

References

Aiuti,A., Webb,I.J., Bleul,C., Springer,T. and Guiterrez-Ramos,J.C. (1996) The chemokine SDF-1 is a chemoattractant for human CD34$^+$ progenitor cells and provides a new mechanism to explain the hemopoietic mobilization of CD34$^+$ progenitors to peripheral blood. *J. Exp. Med.*, **185**, 111–120.

Arenzana-Seisdedos,F., Virelizier,J.-L., Rousset,D., Clark-Lewis,I., Loetscher,P., Moser,B. and Baggiolini,M. (1996) HIV blocked by a chemokine antagonist. *Nature*, **383**, 400.

Baggiolini,M., Dewald,B. and Moser,B. (1997) Human Chemokines: An Update. *Annu. Rev. Immunol.*, **15**, 675–705.

Bleul,C.C., Farzan,M., Choe,H., Parolin,C., Clark-Lewis,I., Sodroksi,J. and Springer,T.A. (1996a) The lymphocyte chemoattractant SDF-1 is a ligand for LESTR/fusin and blocks HIV-1 entry. *Nature*, **382**, 829–833.

Bleul,C.C., Fuhlbrigge,R.C., Casasnovas,J.M., Aiuti,A. and Springer,T.A. (1996b) A highly efficacious lymphocyte chemoattractant, stromal cell-derived factor 1 (SDF-1). *J. Exp. Med.*, **184**, 1101–1109.

Brunger,A.T. (1993) X-PLOR Version 3.1: a system for X-ray crystallography and NMR. Yale University Press, New Haven, USA.

Clark-Lewis,I., Dewald,B., Loetscher,M., Moser,B. and Baggiolini,M. (1994) Structural requirements for interleukin-8 function identified by design of analogs and CXC chemokine hybrids. *J. Biol. Chem.*, **269**, 16075–16081.

Clark-Lewis,I., Kim,K.-S., Rajarathnam,K., Gong,J.-H., Dewald,B., Moser,B., Baggiolini,M. and Sykes,B.D. (1995) Structure–activity relationships of chemokines. *J. Leukocyte Biol.*, **57**, 703–711.

Clavel,F. and Charneau,P. (1994) Fusion from without directed by human immunodeficiency virus particles. *J. Virol.*, **68**, 1179–1185.

Connor,R.I., Sheridan,K.E., Ceradini,D., Choe,S. and Landau,N.R. (1997) Changes in coreceptor use correlates with disease progression in HIV-1 infected individuals. *J. Exp. Med.*, **185**, 621–628.

Fairbrother,W.J. and Skelton,N.J. (1996) Three dimensional structures of the chemokine family. In Horuk,R. (ed.), *Chemoattractant Ligands And Their Receptors*. CRC Press, London, UK, pp. 55–86.

Fairbrother,W.J., Reilly,D., Colby,T., Hesselgesser,J. and Horuk,R. (1994) The solution structure of melanoma growth stimulating activity. *J. Mol. Biol.*, **242**, 252–270.

Farrens,D.L., Altenbach,C., Yang,K., Hubbell,W.L. and Khorana,H.G. (1996) Requirement of rigid-body motion of transmembrane helices for light activation of rhodopsin. *Science*, **274**, 768–770.

Farzan,M., Choe,H., Martin,K.A., Sun,Y., Sidelko,M., Mackay,C.R., Gerard,N.P., Sodroski,J. and Gerard,C. (1997) HIV-1 entry and macrophage inflammatory protein-1 beta-mediated signaling are independent functions of the chemokine receptor CCR5. *J. Biol. Chem.*, **272**, 6854–6857.

Federsppiel,B., Melhado,I.G., Duncan,A.M.V., Delaney,A., Schappert,K., Clark-Lewis,I. and Jirik,F.R. (1993) Molecular cloning of the cDNA and chromosomal localization of the gene for a putative seven-transmembrane segment (7-TMS) receptor isolated from human spleen. *Genomics*, **16**, 707–712.

Feng,Y., Broder,C.C., Kennedy,P.E. and Berger,E.A. (1996) HIV-1 entry cofactor: Functional cDNA cloning of a seven-transmembrane G protein-coupled receptor. *Science*, **272**, 872–877.

Gervaix,A., West,D., Leoni,L.M., Richman,D.D., Wong-Staal,F. and Corbeil,J. (1997) A new reporter cell line to monitor HIV infection and drug susceptibility *in vitro*. *Proc. Natl Acad. Sci. USA*, **94**, 4653–4658.

Gong,J.-H., Uguccioni,M., Dewald,B., Baggiolini,M. and Clark-Lewis,I. (1996) RANTES and MCP-3 antagonists bind multiple chemokine receptors. *J. Biol. Chem.*, **271**, 10521–10527.

Kraulis,P.J. (1991) MOLSCRIPT: A program to produce both detailed and schematic plots of protein structures. *J. Appl. Crystallogr.*, **24**, 946–950.

Lakowski,R.A., MacArthur,M.W., Moss,D.S. and Thornton,J.M. (1991) PROCHECK: A program to check the stereochemical quality of protein structures. *Acta Crystallogr.*, **A47**, 110–119.

LaRosa,G.J., Thomas,K.M., Kaufmann,M.E., Mark,R., White,M., Taylor,L., Gray,G., Witt,D. and Navarro,J. (1992) Amino terminus of the interleukin-8 receptor is a major determinant of receptor subtype specificity. *J. Biol. Chem.*, **267**, 25402–25406.

Loetscher,M., Geiser,T., O'Reilly,T., Zwahlen,R., Baggiolini,M. and Moser,B. (1994) Cloning of a human seven-transmembrane domain receptor, LESTR, that is highly expressed in leukocytes. *J. Biol. Chem.*, **269**, 232–237.

Lowman,H.B., Slagle,P.H., DeForge,L.E., Wirth,C.M., Gillece-Castro,B.L., Bourell,J.H. and Fairbrother,W.J. (1996) Exchanging interleukin-8 and melanoma growth stimulating activity receptor binding specificities. *J. Biol. Chem.*, **271**, 14344–14352.

Merritt,E.A. and Murphy,M.E.P. (1994) Raster3D version 2.0, a program for photorealistic molecular graphics. *Acta Crystallogr.*, **D50**, 869–873.

Monteclaro,F.S. and Charo,I.F. (1996) The amino-terminal extracellular domain of the MCP-1 receptor, but not the RANTES/MIP-1 alpha receptor, confers chemokine selectivity. Evidence for a two-step mechanism for MCP-1 receptor activation. *J. Biol. Chem.*, **271**, 19084–19092.

Nagasawa,T., Kikutani,H. and Kishimoto,T. (1994) Molecular cloning and structure of a pre-B-cell growth-stimulating factor. *Proc. Natl Acad. Sci. USA*, **91**, 2305–2309.

Nagasawa,T., Hirota,S., Tachibana,K., Takakura,N., Nishikawa,S.-I., Kitamura,Y., Yoshida,N., Kikutani,H. and Kishimoto,T. (1996) Defects of B-cell lymphopoiesis and bone-marrow myelopoiesis in mice lacking the CXC chemokine PBSF/SDF-1. *Nature* **382**, 635–638.

Nicholls,A., Sharp,K. and Honig,B. (1991) Protein folding and association: Insights from the interfacial and thermodynamic properties of hydrocarbons. *Proteins*, **11**, 281–296.

Nilges,M., Clore,G.M. and Gronenborn,A.M. (1988) Determination of three-dimensional structures of proteins from interproton distance data by hybrid distance geometry-dynamical simulated annealing calculations. *FEBS Lett.*, **229**, 317–324.

Oberlin,E. *et al.* (1996) The CXC chemokine SDF-1 is the ligand for LESTR/fusin and prevents infection by T-cell-line-adapted HIV-1. *Nature*, **382**, 833–835.

Rajarathnam,K., Clark-Lewis,I. and Sykes,B.D. (1994a) ^{1}H NMR studies of interleukin 8 analogs: Characterization of the domains essential for function. *Biochemistry*, **33**, 6623–6630.

Rajarathnam,K., Sykes,B.D., Kay,C.M., Geiser,T., Dewald,B., Baggiolini,M. and Clark-Lewis,I. (1994b) Neutrophil activation by monomeric interleukin–8. *Science*, **264**, 90–92.

Rajarathnam,K., Clark-Lewis,I. and Sykes,B.D. (1995) ^{1}H NMR solution structure of an active monomeric Interleukin-8. *Biochemistry*, **34**, 12983–12990.

Rot,A. *et al.* (1996) Some aspects of IL-8 pathophysiology. III: Chemokine interaction with endothelial cells. *J. Leukocyte Biol.*, **59**, 39–44.

Shirozu,M., Nakano,T., Inazawa,J., Tashiro,K., Tada,H., Shinohara,T. and Honjo,T. (1995) Structure and chromosomal localization of the human stromal cell-derived factor 1 (SDF1) gene. *Genomics*, **28**, 495–500.

Siciliano,S.J. *et al.* (1994) Two-site binding of C5a by its receptor: an alternative binding paradigm for G protein-coupled receptors. *Proc. Natl Acad. Sci. USA*, **91**, 1214–1218.

Skelton,N.J., Aspiras,F., Ogez,J. and Schall,T.J. (1995) Proton NMR assignments and solution conformation of RANTES, a chemokine of the C-C type. *Biochemistry*, **34**, 5329–5342.

Tashiro,K., Tada,H., Heilker,R., Shirozu,M., Nakano,T. and Honjo,T. (1993) Signal sequence trap: A cloning strategy for secreted proteins and type I membrane proteins. *Science*, **261**, 600–603.

von Tscharner,V., Prod'hom,B., Baggiolini,M. and Reuter,H. (1986) Calcium fluxes and calcium buffering in human neutrophils. *Nature*, **324**, 369–372.

Wuthrich,K. (1986) *NMR of Proteins and Nucleic Acids*. Wiley, NewYork, NY.

Zhang,O., Kay,L.E., Olivier,J.P. and Forman-Kay,J.D. (1994) Backbone ^{1}H and ^{15}N resonance assignments of the N-terminal SH3 domain of drk in folded and unfolded states using enhanced-sensitivity pulsed field gradient NMR techniques. *J. Biomol. NMR*, **4**, 845–858.

Zhang,L., Huang,Y., He,T., Cao,Y. and Ho,D.D. (1996) HIV-1 subtype and second-receptor use. *Nature*, **383**, 768.

Received on July 31, 1997; revised on August 28, 1997